Differential expression profiles of long non-coding RNAs during the mouse pronuclear stage under normal gravity and simulated microgravity

MEIYING FENG[1,2], NANNAN DANG[1,3], YINSHAN BAI[1,4], HENGXI WEI[1], LI MENG[1], KAI WANG[1], ZHIHONG ZHAO[1], YUN CHEN[1], FENGLEI GAO[1,5], ZHILIN CHEN[1,6], LI LI[1] and SHOUQUAN ZHANG[1]

[1]College of Animal Science, National Engineering Research Center for Breeding Swine Industry, Guangdong Provincial Key Lab of Agro-Animal Genomics and Molecular Breeding, College of Animal Science, South China Agricultural University, Guangzhou, Guangdong 510642; [2]College of Life Sciences, Zhaoqing University, Zhaoqing, Guangdong 526061; [3]Department of Reproductive Centre, CALMETTE International Hospital, Kunming, Yunnan 650224; [4]College of Life Science and Engineering, Foshan University, Foshan, Guangdong 528231; [5]College of Tropical Agriculture and Forestry, Guangdong Agriculture Industry Business Polytechnic, Guangzhou, Guangdong 510507; [6]Technology Department, Guangdong Wen's Foodstuffs Group Co., Ltd., Yunfu, Guangdong 527400, P.R. China

Abstract. Pronuclear migration, which is the initial stage of embryonic development and the marker of zygote formation, is a crucial process during mammalian preimplantation embryonic development. Recent studies have revealed that long non-coding RNAs (lncRNAs) serve an important role in early embryonic development. However, the functional regulation of lncRNAs in this process has yet to be elucidated, largely due to the difficulty of assessing gene expression alterations during the very short time in which pronuclear migration occurs. It has previously been reported that migration of the pronucleus of a zygote can be obstructed by simulated microgravity. To investigate pronuclear migration in mice, a rotary cell culture system was employed, which generates simulated microgravity, in order to interfere with murine pronuclear migration. Subsequently, lncRNA sequencing was performed to investigate the mechanism underlying this process. In the present study, a comprehensive analysis of lncRNA profile during the mouse pronuclear stage was conducted, in which 3,307 lncRNAs were identified based on single-cell RNA sequencing data. Furthermore, 52 lncRNAs were identified that were significantly differentially expressed. Subsequently, 10 lncRNAs were selected for validation by reverse transcription-quantitative polymerase chain reaction, in which the same relative expression pattern was observed. The results revealed that 12 lncRNAs (lnc006745, lnc007956, lnc013100, lnc013782, lnc017097, lnc019869, lnc025838, lnc027046, lnc005454, lnc007956, lnc019410 and lnc019607), with tubulin β 4B class IVb or actinin α 4 as target genes, may be associated with the expression of microtubule and microfilament proteins. Binding association was confirmed using a dual-luciferase reporter assay. Finally, Gene Ontology analysis revealed that the target genes of the differentially expressed lncRNAs participated in cellular processes associated with protein transport, binding, catalytic activity, membrane-bounded organelle, protein complex and the cortical cytoskeleton. These findings suggested that these lncRNAs may be associated with migration of the mouse pronucleus.

Introduction

In mice, the pronuclear stage is a vital period in which the activation of zygotic genes begins (1-3). During the pronuclear stage, the zygote undergoes meiosis to form the female pronucleus, and serial reactions in the sperm nucleus occur to form the male pronucleus. In a previous study, it was reported that female and male pronuclear migration in zygotes depends on microtubules and organelles (4,5), and that simulated microgravity, generated by a rotary cell culture system (RCCS), disturbs spindle organization to inhibit mouse oocyte maturation (6), as the microtubules and chromosomes cannot form a complete spindle.

Correspondence to: Professor Shouquan Zhang, College of Animal Science, National Engineering Research Center for Breeding Swine Industry, Guangdong Provincial Key Lab of Agro-Animal Genomics and Molecular Breeding, College of Animal Science, South China Agricultural University, 483 Wushan Road, Tianhe, Guangzhou, Guangdong 510642, P.R. China
E-mail: sqzhang@scau.edu.cn

Long non-coding RNAs (lncRNAs), which evolve rapidly and demonstrate little if any sequence conservation (7), are spliced transcripts that do not encode proteins; lncRNAs range in length from 200 to several thousand nucleotides. Previous studies have reported that there are >1,000 promoter-associated non-coding RNA/gene pairs at the time of zygotic gene activation (ZGA) (8), ~5,563 novel lncRNAs in mouse cleavage-stage embryos (9), and 2,733 novel lncRNAs in human preimplantation embryos, as determined via single-cell RNA sequencing (RNA-Seq) (10). Numerous lncRNAs have been revealed to serve key roles in post-transcriptional, translational and epigenetic regulation, and in embryogenesis without having any apparent function (11-15). Some lncRNAs associate with promoters to activate partner gene expression (8). Previous investigations have mainly focused on early oocytes or later embryonic development, and the global gene expression profiles of lncRNAs have been revealed using single-cell RNA-Seq (10,16-22). However, the biological functions of lncRNAs in mouse pronuclear migration are not well understood.

Although previous studies have investigated whether the disruption of microtubules inhibits pronuclear migration in mouse zygotes, it remains unclear as to whether these microtubular abnormalities are induced by lncRNAs. Therefore, a RCCS was used to generate a model of pronuclear migration defects, and the relative lncRNA expression patterns in the mouse zygote were investigated to understand the biological roles of lncRNAs during pronuclear migration.

Materials and methods

Mouse zygote collection and culture. All animal procedures were carried out according to the guidelines developed by the China Council on Animal Care, and the protocols were approved by the Animal Care and Use Committee of South China Agricultural University (Guangzhou, China). Mice were maintained under the following conditions: Temperature, 18-22°C; humidity, 50-60%; 10-14 h light/dark cycle; *ad libitum* access to food and water. Superovulation of 20 adult female mice (C57BL/6; age, 6-12-weeks; weight, 18-25 g; Guangdong Medical Laboratory Animal Center, Foshan, China) was induced via intraperitoneal injection of 5 IU pregnant mare serum gonadotropin (Ningbo Second Hormone Factory, Ningbo, China), followed by injection of 5 IU human chorionic gonadotropin (hCG; Ningbo Second Hormone Factory) after 48 h. The mice were then placed in individual cages with an adult male mouse (C57BL/6; age, 8-24 weeks; weight, 20-50 g; Guangdong Medical Laboratory Animal Center). The female mice were screened for vaginal plugs the following morning (15 h post-hCG), and mice with vaginal plugs were subsequently dissected for collect ion of their zygotes. A total of 16 h following hCG administration, the zygotes were collected from the ampullae of the oviducts, and the cumulus cells were removed with 300 IU/ml hyaluronidase. The zygotes were subsequently cultured in potassium simplex optimization medium supplemented with a solution of 1% Eagle's Basal Medium and Minimum Essential Media non-essential amino acids, 1% penicillin-streptomycin (Gibco; Thermo Fisher Scientific, Inc., Waltham, MA, UK), 95 mM NaCl, 2.5 mM KCl, 0.35 mM KH_2PO_4, 1.71 mM $CaCl_2$, 25 mM $NaHCO_3$, 1 mM bovine serum albumin, 1 mM glutamine, 0.2 mM pyruvate, 10 mM sodium DL-lactate, 0.2 mM D-glucose, 0.2 mM $MgSO_4$ and 0.01 mM EDTA, and were overlaid with embryo-tested mineral oil in a humidified atmosphere containing 5% CO_2 at 37°C. Unless otherwise specified, all reagents were obtained from Sigma-Aldrich (Merck KGaA, Darmstadt, Germany).

A total of 20 h post-hCG administration, when the pronucleus was observable, the zygotes were randomly divided into two groups (50 zygotes/group). One group was cultured at 37°C in an atmosphere containing 5% CO_2 under normal gravity for 9 h (three repetitions, groups C1, C2 and C3), after which, the zygotes (in which the pronuclei were adjacent to each other) were collected immediately. The other group was cultured at 37°C in an atmosphere containing 5% CO_2 in the RCCS (Synthecon Inc., Houston, TX, USA), under simulated microgravity for 9 h, as described previously (three repetitions, groups R1, R2 and R3) (6). The zygotes exhibiting disrupted pronuclear migration were collected immediately. Zygotes collected from the two groups were transferred to 80 μl RNA extraction buffer (Qiagen RNeasy Mini kit; Qiagen, Inc., Valencia, CA, USA) for RNA isolation and were stored at -80°C until sequencing.

Immunofluorescence and laser-scanning confocal microscopy. The immunohistochemical assay was performed as previously described (6). Zygotes were fixed with 4% paraformaldehyde for 30 min at room temperature, blocked in 1% bovine serum albumin (BSA; Sigma-Aldrich; Merck KGaA) for 30 min at room temperature, and incubated with a mouse monoclonal anti-α-tubulin antibody (1:200; cat. no. T8328; Sigma-Aldrich; Merck KGaA) at 4°C overnight. Zygotes were washed three times in washing buffer (6), including 0.02% NaN_3 (20 mg/ml), 0.01% Triton-X, 0.2% non-fat dry milk, 2% normal goat serum (cat. no. AR0009; Wuhan Boster Biological Technology, Ltd., Wuhan, China), 0.1 M glycine, 2% BSA and 95.77% PBS, prior to each step. The zygotes were sequentially incubated with an Alexa Fluor® 568-labelled goat anti-mouse immunoglobulin G secondary antibody (1:100; cat. no. A11031; Invitrogen; Thermo Fisher Scientific, Inc.) for 1 h at 37°C in the dark. Finally, the zygotes were washed, stained with 10 μg/ml Hoechst 33342 (Molecular Probes; Thermo Fisher Scientific, Inc.) for 10 min at 37°C in the dark to detect DNA, mounted in PBS containing 50% glycerol (anti-fading reagent) and 25 mg/ml NaN_3, and then examined with a Zeiss laser-scanning confocal microscope (Carl Zeiss AG, Oberkochen, Germany).

Single-cell cDNA amplification and RNA-Seq library preparation. To prepare single-cell cDNA, all the samples were amplified using the Smart-Seq2 method (23), and a cDNA product of 1-2 kb in length was obtained. Subsequently, single-cell cDNA was purified with the Ampure XP kit (Beckman Coulter, Inc., Brea, CA, USA). The concentration and fragment distribution of the single-cell cDNA obtained from normal gravity and simulated microgravity zygote samples were subsequently assessed in a Qubit® 3.0 fluorometer (Thermo Fisher Scientific, Inc.), and the High Sensitivity DNA Assay kit in the Bioanalyzer 2100 system (Agilent Technologies, Inc., Santa Clara, CA, USA).

Single-cell cDNA (20 ng) was used as the initial material for library construction. Initially, a Bioruptor® Sonication system (20-60 kHz; 4˚C; 30 sec; Diagenode, Inc., Denville, NJ, USA) was employed to generate small fragments ~300 bp in length. Subsequently, the library fragments were subjected to end repair via the addition of a poly(A) tail and an adapter sequence. The Beckman Ampure XP kit was used to purify fragments after each reaction. Polymerase chain reaction (PCR) was subsequently performed, and different index tags, which were used for distinguishing samples from each other during sequencing, were added to each sample. The PCR products were retrieved via 2% agarose gel electrophoresis in order to select for 4,000-bp DNA fragments, from which the library was constructed. The Agilent Bioanalyzer 2100 system (Agilent Technologies, Inc.) was then used to assess the quality of the libraries.

Deep sequencing and expression analysis of lncRNAs. The libraries were sequenced on the Illumina HiSeq 2500 platform (Illumina, Inc., San Diego, CA, USA) using 150-bp paired-end sequencing. Sequencing reads were assessed with the FASTX tool kit (http://hannonlab.cshl.edu/fastx_toolkit/) and were then subjected to standard quality control criteria to remove short (<30 bp) and low-quality (quality score <20) reads. After trimming the adaptor sequences, high-quality clean reads were obtained for the following analysis. Firstly, the reads were mapped to the mouse reference genome (mm9; genome.ucsc.edu/) with TopHat v1.4.0 software, assembled with Cufflinks v2.2.0 and annotated with RefSeq (www.ncbi. nlm.nih.gov/refseq) to remove the annotated genes known to encode proteins or small RNAs (24). Genes/transcripts with fragments per kilobase transcriptome per million reads (FPKM) >10 were retained, meaning that if there was only one exon, the length could be >2,000 bp, whereas if more than two exons were present, the length could be >200 bp. The coding potential of the transcripts was then identified by CPC 2.0 software; subsequently, transcripts with coding potential were excluded, and the final lncRNAs were obtained (25). Finally, the read counts for each novel transcript were converted into FPKM, values which were used to calculate gene expression.

Screening and cluster analysis of differentially expressed lncRNAs. Differences in the expression of the lncRNAs were calculated based on the *Q*-value, and genes with similar expression patterns were directly reflected in the cluster analysis conducted using the hierarchical complete linkage clustering method in R software (R version 3.4.3; www.r-project.org/). Significant differences in lncRNA expression levels were determined based on a *Q*-value cut-off 0.05 and a minimum fold change (FC) of 1.5 using DEseq software package version: 1.20.0 (26). The differentially expressed lncRNAs were replaced by log10 values (data values), and the Euclidean distance was calculated. The results were further analysed using R packages; specifically, the 'heatmap 2' function of the 'gplots' package, which was used to draw heat maps of the differentially expressed lncRNAs.

Reverse transcription-quantitative PCR (RT-qPCR) and statistical analysis. RT-qPCR was performed to validate the RNA-Seq results for lncRNA expression. Total RNA was extracted from 100 fertilized embryos using the Qiagen RNeasy Mini kit (Qiagen, Inc.), according to the manufacturer's protocol. RNA then underwent RT using the PrimeScript™ RT Reagent kit with gDNA Eraser (perfect real time; Takara Bio, Inc., Otsu, Japan). The relative expression levels of the target lncRNAs were measured by RT-qPCR using the Power SYBR-Green RT-PCR kit (Toyobo Life Science, Osaka, Japan) in a Bio-Rad CFX96 PCR system (Bio-Rad Laboratories, Inc., Hercules, CA, USA). H2A histone family member Z was employed as a housekeeping gene, and each sample was analysed three times. The lncRNA-specific PCR conditions were as follows: Initial denaturation at 95˚C for 5 min, followed by 40 cycles of denaturation at 95˚C for 10 sec, annealing at 60˚C for 10 sec and extension at 72˚C for 30 sec. RT-qPCR primers used in these analyses are presented in Table I.

The comparative quantification cycle (Cq) method was employed to quantify the relative expression of lncRNAs. The expression levels of the lncRNAs were analysed as FC values using the ΔCq method (27). All data were log transformed, and the results were comparable to the RNA-Seq data.

Analysis of functional enrichment and the lncRNA-gene network. BLAST v2.2.24 (https://blast.ncbi.nlm.nih. gov/Blast.cgi) and RNAplex software (https://omictools. com/rnaplex-tool) were used to predict and identify the target genes (mRNAs) of the lncRNAs, whereas Cytoscape V3.6.1 software was used to construct the lncRNA-gene network (28). The stage-specific lncRNAs, showing differential expression between the two groups, and their target genes were chosen to construct the network. For further analysis, tubulin β-4B class IVb (*Tubb4b*) and lnc007956 were chosen to validate the association between a target gene and lncRNA. However, it is difficult to induce gene transfer in early embryos. The 293FT cell line has the advantage of easier culture, higher transfer efficiency and easier experimental operation; it is usually used to verify the target association of microRNA/lncRNAs in mammalian cells (29). In the present study, 293FT cells (cat. no. R70007; Thermo Fisher Scientific), which were grown to 70-80% confluence in 96-well plates, were co-transfected with a dual-luciferase reporter (cat. no. E1330; Promega Corporation, Madison, WI, USA) carrying wild-type or mutant *Tubb4b* (sequence was mutated from 5'-TGGTGCCCT TCCCTCGCCTGCACTTCTTCATGCC-3' to 5'-TGGTGC ACTTCACTCGCCTGCACGTCTGCATATC-3'; 100 ng) and a plasmid carrying the lncRNA [100 ng; pcDNA3.1(-), cat. no. V795-20; Invitrogen; Thermo Fisher Scientific, Inc.] using Lipofectamine® 3000 (Invitrogen; Thermo Fisher Scientific, Inc.) at 37˚C in an atmosphere containing 5% CO_2 for 24 h. Luciferase activity was measured using the Dual-Luciferase Reporter Assay system (Promega Corporation) and compared with *Renilla* luciferase activity, according to the manufacturer's protocol 36 h post-transfection. This experiment was repeated more than three times and results were analysed using a Student's t-test (Microsoft Excel 2010; Microsoft Corporation, Redmond, WA, USA). P<0.05 was considered to indicate a statistically significant difference.

LncRNA functions were predicted based on the corresponding target genes through Gene Ontology (GO) analysis. GO enrichment in terms of molecular function, cellular component and biological process categories was

Table I. Primer sequences of the lncRNAs and housekeeping gene for reverse transcription-quantitative polymerase chain reaction.

Gene lncRNA	Primer sequence (5'-3')	Product length (bp)
H2afz	F: ACAGCGCAGCCATCCTGGAGTA	202
	R: TTCCCGATCAGCGATTTGTGGA	
lnc013878	F: ACCTGTGCCAAATGAGGCTT	181
	R: CTGCCAGTGTCTAAGGTGCT	
lnc019773	F: GTCAGCTCTACAACCGCAGA	182
	R: TCCCGGTATTTAGGAGGGGG	
lnc025630	F: TCAATGTCTGAATCGCCAACC	160
	R: GCATGGTGACAGCTTTTCATAATAC	
lnc023277	F: GCGAGCCTTCCCGTTATCAT	116
	R: TACTGCGGCGTTTCCTTCTC	
lnc013100	F: GTGGCTTGCTCATACCAGGA	149
	R: GTTTTGTGCAGAGCCATCCC	
lnc019410	F: CCGGTTTATCCACGTCTGCT	115
	R: GAACATCACTTGTGGCAGCG	
lnc032797	F: TGTTGTAACGGAGCACCTGAT	104
	R: AATCCCAGACGACTCCGGT	
lnc006988	F: ACGGGCTCATCATTATCACTCTG	109
	R: TTCATGGGAGGTTGGCAGTAA	
lnc001078	F: ACCAGTTTGTTTCTCTGTTGATGC	124
	R: CCTTCAGTGTCCCTGTTCCCT	
lnc007956	F: TCTTCCTCTCGCCCCTAGTC	100
	R: ATCTGAGCTTCTCAACCCTGG	

F, forward; *H2afz*, H2A histone family member Z; lnc, long non-coding; R, reverse primer.

assessed using the MGI Goslim Database (www.informatics. jax.org/gotools/MGI_GO_Slim.html) and the R package GSEABase. The most enriched terms may reflect lncRNA functions. Hypergeometric tests with the Benjamini and Hochberg false discovery rate were performed using the default parameters in order to adjust the Q-value.

Results

Simulated microgravity negatively affects mouse pronuclear migration. To investigate the effects of simulated microgravity on mouse pronuclear migration, zygotes in which the male and female pronuclei were forming were cultured for spontaneous maturation under RCCS (Fig. 1A) or normal gravity (Fig. 1B) conditions for 9 h. Subsequently, the zygotes cultured under simulated microgravity were cultured at 37°C in an atmosphere containing 5% CO_2 under normal gravity for 10 h (Fig. 1C) and 40 h, whereas the culture conditions for the control group were unchanged. Subsequently, for each group, the proportions of complete pronuclear migration, and of embryos at the 2-cell and 4-cell stages, were recorded following the onset of embryonic development (Table II). During further culture, the control zygotes exhibited orderly embryonic development (Fig. 1D), whereas those in the simulated microgravity group were stalled at the pronuclear merge stage (Fig. 1C). The zygotes cultured in the RCCS completed pronuclear migra-tion after 10 h under normal gravity (Fig. 1C) but could not progress to the 2-cell stage (Table II). The present study further investigated whether tubulin protein expression was altered in the two groups using immunofluorescence; tubulin protein was disturbed in the RCCS group (Fig. 1E-G) compared with in the control group (Fig. 1H-J), which tubulin protein had assembled nearby the male and female pronuclei. Pronuclear migration was markedly compromised when zygotes were cultured under simulated microgravity conditions, and altera-tions in the configuration of microtubules were observed after staining for tubulin protein (Fig. 1E-J).

RNA-Seq and lncRNA data for mouse zygotes during the pronuclear stage. The Illumina HiSeq 2500 platform was used to perform RNA-Seq on the six cDNA libraries (groups C1, C2, C3, R1, R2 and R3), and 125-bp paired-end reads were generated. The number of raw reads was >40 million (Table III). Low-quality reads were filtered, and the clean reads still included >81.58% of the raw data. Among the clean reads, 92.29% exhibited perfect BLAST hits against the mouse reference genome (https://blast.ncbi.nlm.nih.gov/Blast.cgi), and >85.19% of the total mapped reads were uniquely mapped (Table III), indicating that the data were credible and could be used for further analyses.

After the removal of protein-coding genes and transcripts that were <200 bp, a total of 6,254 novel lncRNA transcripts were obtained from the 3,307 expressed loci in the RNA-Seq analysis. The lncRNAs varied between 200 and 7,804 bp
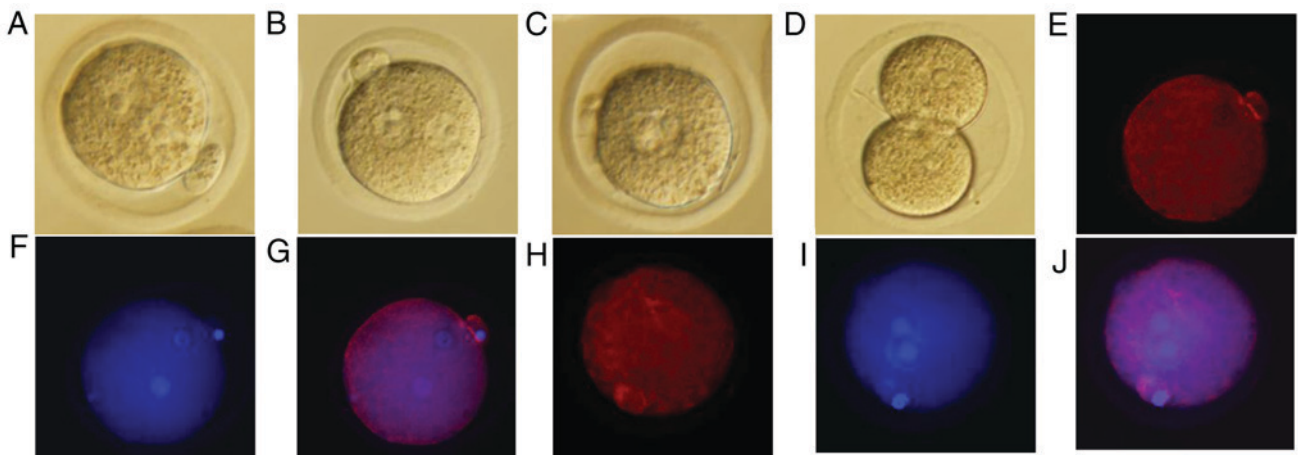
Figure 1. Representative images of mouse embryos at various stages under the different culture conditions (magnification, x200). (A) Unassembled stage of the male and female pronuclei under simulated microgravity from the RCCS group. (B) Assembly of male and female pronuclei from the control group. (C) Fusion of the male and female pronuclei after 10 h of culture without simulated microgravity from the RCCS group. (D) Embryos at the 2-cell stage after 19 h of culture in potassium simplex optimized medium from the control group. Samples in (A) and (B) were cultured at the same time, as were those in (C) and (D) (E) Immunofluorescence staining of tubulin in the mouse zygote under simulated microgravity. (F) Immunofluorescent Hoechst 33342 staining in the mouse zygote under simulated microgravity. (G) Merge of (E) and (F) images. (H) Immunofluorescence staining of tubulin in the mouse zygote under normal gravity. (I) Immunofluorescent Hoechst 33342 staining in the mouse zygote under normal gravity. (J) Merge of (H) and (I) images. RCCS, rotary cell culture system.

in length, with 45.8% falling between 200 and 1,000 bp, 36.3% between 1,000 and 2,000 bp, 13.1% between 2,000 and 3,000 bp, 4.4% between 3,000 and 5,000 bp, and 0.4% between 5,000 and 10,000 bp (Fig. 2A). The lncRNA genes had an average length of 1,305 bp, and the lncRNA transcripts were mainly located on mouse chromosomes 1-19 and X (Fig. 2B). Therefore, the existence of a large number of lncRNA transcripts at the mouse pronuclear stage was confirmed.

Differential expression analysis of lncRNAs. To analyse the differential expression of lncRNAs in mouse zygotes between the normal gravity and simulated microgravity culture conditions, lncRNA sequencing was performed to explore the key lncRNAs during mouse pronuclear migration. A total of 52 lncRNAs were significantly differentially expressed between the control and RCCS groups in the mouse zygotes, and unsupervised hierarchical clustering and scatterplot analysis (FC>1.5 and P<0.05) based on the FPKM values (log2 transformed) were conducted to select the key lncRNAs that affect mouse pronuclear migration (Fig. 3A and B). Compared with in the control group, the RCCS group included 19 lncRNAs that were upregulated and 33 lncRNAs that were downregulated (data not shown).

Verification through RT-qPCR. To validate the RNA-Seq results for lncRNA expression levels, 10 differentially expressed lncRNAs (lnc013878, lnc019773, lnc025630, lnc023277, lnc013100, lnc019410, lnc032797, lnc006988, lnc001078 and lnc007956) were selected for testing in mouse zygotes using RT-qPCR. The RT-qPCR results confirmed that the expression patterns were similar to those obtained via RNA-Seq (Fig. 3C). These results indicated that the RNA-Seq data were credible and could be used to study pronuclear migration in the mouse zygote.

LncRNA-gene interaction network analysis. In the present study, the target genes (mRNAs) of the differentially expressed lncRNAs were predicted and identified using BLAST and RNAplex software, in order to investigate the function of the lncRNAs regulating mouse pronuclear migration (30). Subsequently, a lncRNA-gene interaction network between differentially expressed lncRNAs and their target genes was constructed with Cytoscape software. A total of 668 network nodes (40 lncRNAs and 628 protein-coding genes) and 2,289 lncRNA-gene connections were identified in the network (data not shown). Furthermore, 12 lncRNA-gene pairs [lnc006745-actinin-α4 (*Actn4*), lnc007956-*Actn4*, lnc013100-*Actn4*, lnc013782-*Actn4*, lnc017097-*Actn4*, lnc019869-*Actn4*, lnc025838-*Actn4*, lnc027046-*Actn4*, lnc005454-*Tubb4b*, lnc007956-*Tubb4b*, lnc019410-*Tubb4b* and lnc019607-*Tubb4b*] that may be associated with pronuclear migration were identified (Fig. 4A).

To further determine whether lnc007956 binds directly to *Tubb4b*, two dual-luciferase reporter vectors were constructed, with the wild-type or mutant target sequence of *Tubb4*, inserted at the 3' end of the firefly luciferase gene. Subsequently, the effects of lnc007956 on these reporters in 293FT cells were tested. The results demonstrated that lnc007956 transfection significantly inhibited reporter activity (P<0.01), whereas there was no effect on mutant reporter activity (Fig. 4B), suggesting that the predicted binding site in *Tubb4b* is a bona fide target of lnc007956.

GO analysis. To investigate the functions of the lncRNAs in mouse early embryonic development, the target genes of the differentially expressed lncRNAs were enriched through GO analysis. Based on this analysis, 39 enriched GO terms potentially associated with biological processes, 18 enriched GO terms potentially associated with molecular functions and 67 enriched GO terms potentially associated with cellular components were identified. Additionally, 15 GO terms, including cellular process, protein transport, binding, catalytic activity, membrane-bounded organelle, protein complex and cortical cytoskeleton, were significantly associated with mouse pronuclear migration (Fig. 4C).

Table II. *In vitro* development of the embryos under different culture conditions.

Group	Number of cultured zygotes	Rate of development at the indicated stage (%)		
		Completed migration	2-cell stage	4-cell stage
Control	292	100.00	90.75	52.74
RCCS	257	78.21[a]	0.79[b]	0.00[b]

Number of replicates, ≥3. [a]P<0.05 and [b]P<0.001 vs. the control group. RCCS, rotary cell culture system.

Table III. Summary of the draft reads of the six libraries obtained via RNA sequencing.

Sample	Raw reads	Clean reads (%)	Mapped reads (%)	Unique mapped reads (%)
Control 1	47,771,190	43,350,036 (90.75)	41,613,034 (95.99)	37,050,242 (89.04)
Control 2	54,131,806	45,000,374 (83.13)	43,786,923 (97.30)	39,498,918 (90.21)
Control 3	64,009,546	52,978,050 (82.77)	51,500,762 (97.21)	46,592,730 (90.47)
RCCS 1	49,911,144	42,055,314 (84.26)	40,902,021 (97.26)	36,680,028 (89.68)
RCCS 2	61,916,186	51,834,282 (83.72)	47,837,489 (92.29)	40,753,247 (85.19)
RCCS 3	57,604,508	46,994,506 (81.58)	45,471,826 (96.76)	41,184,968 (90.57)

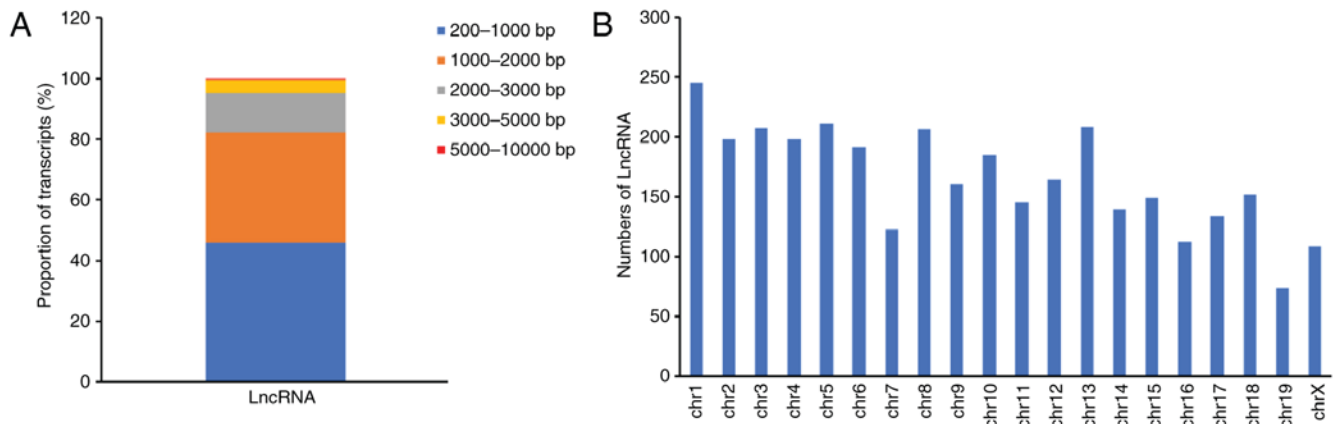RCCS, rotary cell culture system.

Figure 2. Characteristics of mouse pronuclear lncRNAs. (A) Length distribution of mouse pronuclear lncRNAs. (B) Chromosomal distribution of the mouse pronuclear lncRNAs. chr, chromosome; lncRNA, long non-coding RNA.

Discussion

In mice, the completion of pronuclear migration is a crucial step in ZGA and serves an important role in development of the early embryo. To generate a model of pronuclear migration defects, in order to evaluate the role of pronuclear progression during early embryonic development, an RCCS was used to simulate microgravity conditions in a previous study and was revealed to inhibit polar body extrusion by disrupting microtubule organization during mouse oocyte maturation (6). To investigate the progress of pronuclear migration, simulated microgravity was used to alter the organization of the microtubules in mouse zygotes and it was demonstrated that zygotes cultured under simulated microgravity exhibit a delay in the assembly of male and female pronuclei, and that progression to the 2-cell stage is also affected. As ZGA begins approximately at the pronuclear stage and transcription of a wide variety of transcripts occurs at the 2-cell stage in mice (1,2), zygotes with defects in pronuclear migration may possess altered activation of specific genes at the pronuclear stage, which are required for progression to the 2-cell stage. The present results suggested that simulated microgravity altered gene expression in mouse zygotes to prevent progression to the 2-cell stage; therefore, zygotes cultured in the RCCS represent a good model for studying the impact of pronuclear migration in mice.

Increasing number of mRNA and lncRNA expression profiles during early embryonic development have been obtained via single-cell RNA-Seq (10), and the molecular
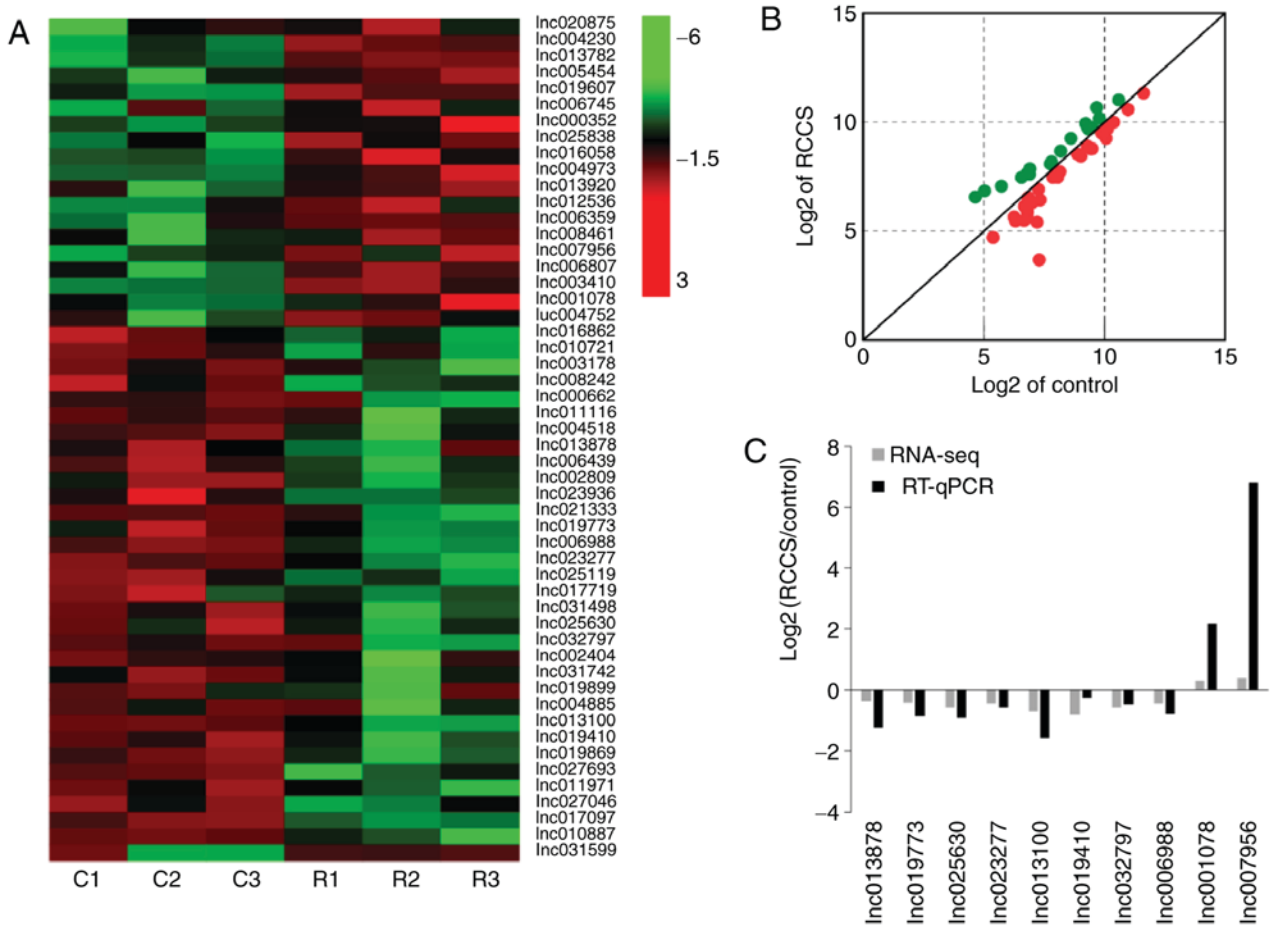
Figure 3. Expression profiles and RNA-Seq analysis of differentially expressed lncRNAs during the pronuclear stage in mouse zygotes. (A) Clustered heatmaps of lncRNAs showing differential expression between mouse zygotes in the control and RCCS groups (FC>1.5 and P<0.05); the number of lncRNAs is shown on the right. Red indicates high relative expression, and green indicates low relative expression. (B) Scatterplot of lncRNA expression. (C) Results of RNA-Seq and RT-qPCR analyses between the control and RCCS groups. Black indicates the results of RT-qPCR, whereas grey indicates the results of RNA-Seq. C corresponds to the fertilized zygotes cultured under normal gravity (Control), and R corresponds to the fertilized zygotes cultured under simulated microgravity (rotary cell culture system). lnc/lncRNA, long non-coding RNA; RNA-Seq, RNA sequencing; RT-qPCR, reverse transcription-quantitative polymerase chain reaction.

mechanisms by which many of these RNAs modulate early embryonic development have been elucidated (20,31,32). However, whether alterations in genes associated with pronuclear migration are regulated by mRNA/lncRNAs remains unknown. Based on the high resolution of RNA-Seq, single-cell RNA-Seq can be used to examine rare cell types, identify molecules of low abundance, capture brief events and detect weak associations masked in bulk experiments (33,34). Therefore, single-cell RNA-Seq represents a promising tool for exploring the expression levels of lncRNAs in mouse pronuclear migration; this approach was used in the present study to elucidate the lncRNA profile during mouse pronuclear migration and identified 6,254 novel lncRNA transcripts from the 3,307 expressed loci. In addition, previous studies identified 5,563 novel lncRNAs in mouse cleavage-stage embryos (9), and 2,733 novel lncRNAs in human preimplantation embryos (10), thus confirming that there are numerous lncRNAs present during early mammalian embryonic development and that lncRNAs may serve a vital role in the pronuclear stage. Through further investigation, 52 differentially expressed lncRNAs were identified and 10 of these lncRNAs were selected to validate the accuracy of the RNA-Seq results

via RT-qPCR. The RT-qPCR results were concordant with the RNA-Seq results, demonstrating that the results of single-cell RNA-Seq were reliable.

It remains unclear as to how many lncRNAs are involved in mouse pronuclear migration. Therefore, the functions of lncRNAs were predicted based on their association with known protein-coding genes and a lncRNA-target gene co-expression network was constructed. Subsequently, based on the identification of *Tubb4b* and *Actn4* as target genes, 12 lncRNAs linked to microfilaments and microtubules were identified, which may affect mouse pronuclear migration. It has been reported that microfilaments and microtubules are essential proteins for male and female pronuclei (3,35-37). During mouse pronuclear migration, specific tools and associated proteins (such as microfilaments and microtubules) become activated, and the sperm centrosome forms a sperm aster, to bring the male and female pronuclei together to complete migration (3,37).

Tubulins, which include eight α and nine β isotypes, are the proteins that form microtubules, which are cytoskeletal elements of all eukaryotic cells that participate in various essential cellular functions (38). *Tubb4b*, also referred to as the tubulin β-2C chain, is tightly associated
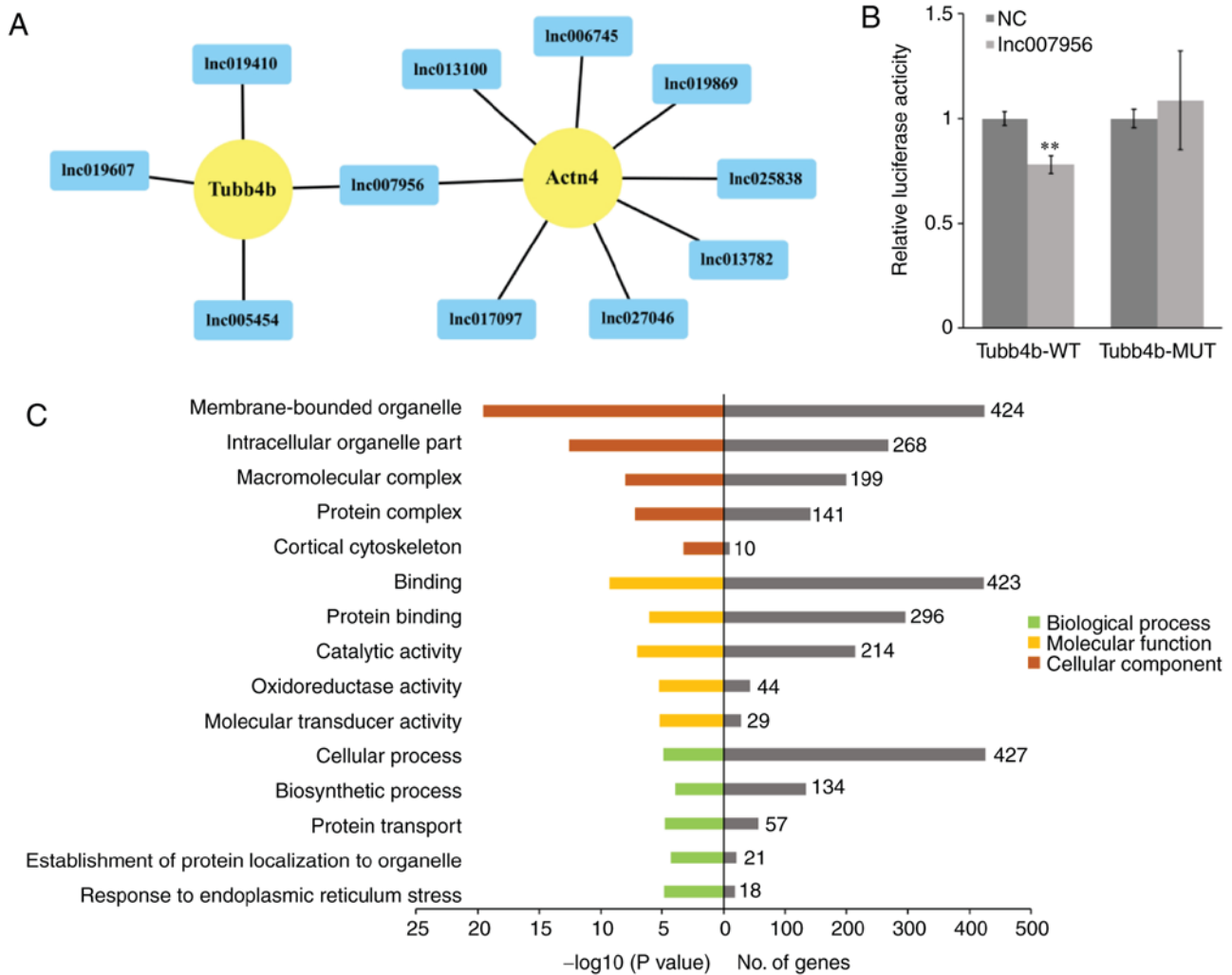
Figure 4. LncRNA-gene network and GO analysis of differentially expressed lncRNAs. (A) Network of 12 lncRNA-gene pairs associated with mouse pronuclear migration. The target genes are displayed as yellow circles, and the differentially expressed lncRNAs are displayed as blue rectangles. (B) Dual-luciferase reporter assay for lnc007956 and *Tubb4b*. **P<0.01 vs. NC. (C) GO term analysis for the target genes of the differentially expressed lncRNAs. Bar plots showing GO enrichment in various modules. The length of the bars indicates significance (left side, -log10 transformed Benjamini-Hochberg adjusted *Q*-value) and the target gene count (right side). *Actn4*, actinin-α4; GO, Gene Ontology; lnc/lncRNA, long non-coding RNA; MUT, mutant; NC, normal control; *Tubb4b*, tubulin β-4B class IVb; WT, wild-type.

with active spermatogenesis in mice (39). *Actn4* belongs to the α-actinin family of cytoskeletal proteins that display unique characteristics associated with cytoskeletal organization, signal transduction, regulation of gene expression, protecting cells from mechanical stress and controlling cell movement (40-42). Knockdown of *Actn4* expression in keratinocytes and murine lung fibroblasts not only impairs the directionality of cell migration but also reduces cell proliferation (43,44). In the dual-luciferase reporter assay, lnc007956 was revealed to bind to the predicted binding site in *Tubb4b* mRNA, thus indicating that lnc007956 may regulate mouse pronuclear migration by binding to *Tubb4b*. Therefore, lncRNAs may be considered to regulate mouse pronuclear migration, and lncRNA defects could result in abnormalities of microtubules and microfilaments.

According to GO analysis, lncRNA target genes were independently enriched in cellular process-associated terms, including protein transport, binding, catalytic activity, membrane-bounded organelle, protein complex and cortical cytoskeleton. In *Caenorhabditis elegans* embryos, migration

of the female pronucleus is associated with organelles, which promote the movement of the female pronucleus along the microtubules to the sperm centrosome (35,36). LncRNAs may control the molecules involved in this process in mice, thereby affecting mouse pronuclear migration. Notably, these data greatly improve the understanding of early embryonic development and may lead to the development of highly efficient markers for analysing the molecular mechanisms of zygote pronuclear migration. The present study provided basic data, which may improve the treatment of physiological reproductive disorders.

Availability of data and materials

The datasets used and/or analysed during the current study are available from the corresponding author on reasonable request. The datasets generated and/or analysed during the current study are also available in the Gene Expression Omnibus repository, https://www.ncbi.nlm.nih.gov/geo/query/acc.cgi?acc=GSE118001

Authors' contributions

MF designed the study, performed the experiments, analyzed the data, and wrote the manuscript. ND collected zygotes from the two groups and recorded the number of embryos at the 2-cell and 4-cell stages. YB participated in the cell culture experiments. KW and ZZ collected and analyzed the data. HW and LM provided guidance with regards to the experiments and analytical methods, analyzed the data, revised the manuscript, and provided administrative and financial support; YC, ZC, FG and LL were responsible for collection and assembly of data. SZ conceived the idea, designed the experiments, provided administrative and financial support, and gave final approval of the manuscript. All authors read and approved the final manuscript.

Ethics approval and consent to participate

All animal procedures were carried out according to the guidelines developed by the China Council on Animal Care, and the protocols were approved by the Animal Care and Use Committee of Guangdong Province, China.

Patient consent for publication

Not applicable.

Competing interests

The authors declare that they have no competing interests.

References

1. Aoki F, Worrad DM and Schultz RM: Regulation of transcriptional activity during the first and second cell cycles in the preimplantation mouse embryo. Dev Biol 181: 296-307, 1997.
2. Latham KE, Garrels JI, Chang C and Solter D: Quantitative analysis of protein synthesis in mouse embryos. I. Extensive reprogramming at the one- and two-cell stages. Development 112: 921-932, 1991.
3. Gundersen GG and Worman HJ: Nuclear positioning. Cell 152: 1376-1389, 2013.
4. Clift D and Schuh M: Restarting life: Fertilization and the transition from meiosis to mitosis. Nat Rev Mol Cell Biol 14: 549-562, 2013.
5. Schatten G, Simerly C and Schatten H: Microtubule configurations during fertilization, mitosis, and early development in the mouse and the requirement for egg microtubule-mediated motility during mammalian fertilization. Proc Natl Acad Sci USA 82: 4152-4156, 1985.
6. Wu C, Guo X, Wang F, Li X, Tian XC, Li L, Wu Z and Zhang S: Simulated microgravity compromises mouse oocyte maturation by disrupting meiotic spindle organization and inducing cytoplasmic blebbing. PLoS One 6: e22214, 2011.
7. Kutter C, Watt S, Stefflova K, Wilson MD, Goncalves A, Ponting CP, Odom DT and Marques AC: Rapid turnover of long noncoding RNAs and the evolution of gene expression. PLoS Genet 8: e1002841, 2012.
8. Hamazaki N, Uesaka M, Nakashima K, Agata K and Imamura T: Gene activation-associated long noncoding RNAs function in mouse preimplantation development. Development 142: 910-920, 2015.
9. Zhang K, Huang K, Luo Y and Li S: Identification and functional analysis of long non-coding RNAs in mouse cleavage stage embryonic development based on single cell transcriptome data. BMC Genomics 15: 845, 2014.
10. Yan L, Yang M, Guo H, Yang L, Wu J, Li R, Liu P, Lian Y, Zheng X, Yan J, et al: Single-cell RNA-Seq profiling of human preimplantation embryos and embryonic stem cells. Nat Struct Mol Biol 20: 1131-1139, 2013.
11. Wang KC and Chang HY: Molecular mechanisms of long noncoding RNAs. Mol Cell 43: 904-914, 2011.
12. Mercer TR, Dinger ME and Mattick JS: Long non-coding RNAs: Insights into functions. Nat Rev Genet 10: 155-159, 2009.
13. Mercer TR and Mattick JS: Structure and function of long noncoding RNAs in epigenetic regulation. Nat Struct Mol Biol 20: 300-307, 2013.
14. Ulitsky I and Bartel DP: lincRNAs: Genomics, evolution, and mechanisms. Cell 154: 26-46, 2013.
15. Pauli A, Rinn JL and Schier AF: Non-coding RNAs as regulators of embryogenesis. Nat Rev Genet 12: 136-149, 2011.
16. Hamatani T, Carter MG, Sharov AA and Ko MS: Dynamics of global gene expression changes during mouse preimplantation development. Dev Cell 6: 117-131, 2004.
17. Wang QT, Piotrowska K, Ciemerych MA, Milenkovic L, Scott MP, Davis RW and Zernicka-Goetz M: A genome-wide study of gene activity reveals developmental signaling pathways in the preimplantation mouse embryo. Dev Cell 6: 133-144, 2004.
18. Xie D, Chen CC, Ptaszek LM, Xiao S, Cao X, Fang F, Ng HH, Lewin HA, Cowan C and Zhong S: Rewirable gene regulatory networks in the preimplantation embryonic development of three mammalian species. Genome Res 20: 804-815, 2010.
19. Tang F, Barbacioru C, Nordman E, Bao S, Lee C, Wang X, Tuch BB, Heard E, Lao K and Surani MA: Deterministic and stochastic allele specific gene expression in single mouse blastomeres. PLoS One 6: e21208, 2011.
20. Li XY, Cui XS and Kim NH: Transcription profile during maternal to zygotic transition in the mouse embryo. Reprod Fertil Dev 18: 635-645, 2006.
21. Tang F, Barbacioru C, Wang Y, Nordman E, Lee C, Xu N, Wang X, Bodeau J, Tuch BB, Siddiqui A, et al: mRNA-Seq whole-transcriptome analysis of a single cell. Nat Methods 6: 377-382, 2009.
22. Fan X, Zhang X, Wu X, Guo H, Hu Y, Tang F and Huang Y: Single-cell RNA-seq transcriptome analysis of linear and circular RNAs in mouse preimplantation embryos. Genome Biol 16: 148, 2015.
23. Serra L, Chang DZ, Macchietto M, Williams K, Murad R, Lu D, Dillman AR and Mortazavi A: Adapting the smart-seq2 protocol for robust single worm RNA-seq. Bio Protoc 8: e2729, 2018.
24. Trapnell C, Roberts A, Goff L, Pertea G, Kim D, Kelley DR, Pimentel H, Salzberg SL, Rinn JL and Pachter L: Differential gene and transcript expression analysis of RNA-seq experiments with TopHat and Cufflinks. Nat Protoc 7: 562-578, 2012.
25. Kong L, Zhang Y, Ye ZQ, Liu XQ, Zhao SQ, Wei L and Gao G: CPC: Assess the protein-coding potential of transcripts using sequence features and support vector machine. Nucleic Acids Res 35: W345-W349, 2007.
26. Love MI, Huber W and Anders S: Moderated estimation of fold change and dispersion for RNA-seq data with DESeq2. Genome Biol 15: 550, 2014.
27. Livak KJ and Scmittgen TD: Analysis of relative gene expression data using real-time quantitative PCR and the 2(-Delta Delta C(T)) method. Methods 25: 402-408, 2001.
28. Shannon P, Markiel A, Ozier O, Baliga NS, Wang JT, Ramage D, Amin N, Schwikowski B and Ideker T: Cytoscape: A software environment for integrated models of biomolecular interaction networks. Genome Res 13: 2498-2504, 2003.

29. Wu GQ, Wang X, Zhou HY, Chai KQ, Xue Q, Zheng AH, Zhu XM, Xiao JY, Ying XH, Wang FW, *et al*: Evidence for transcriptional interference in a dual-luciferase reporter system. Sci Rep 5: 17675, 2015.
30. Tafer H and Hofacker IL: RNAplex: A fast tool for RNA-RNA interaction search. Bioinformatics 24: 2657-2663, 2008.
31. Cote I, Vigneault C, Laflamme I, Laquerre J, Fournier E, Gilbert I, Scantland S, Gagne D, Blondin P and Robert C: Comprehensive cross production system assessment of the impact of in vitro microenvironment on the expression of messengers and long non-coding RNAs in the bovine blastocyst. Reproduction 142: 99-112, 2011.
32. Plourde D, Vigneault C, Lemay A, Breton L, Gagne D, Laflamme I, Blondin P and Robert C: Contribution of oocyte source and culture conditions to phenotypic and transcriptomic variation in commercially produced bovine blastocysts. Theriogenology 78: 116-131, 2012.
33. Shalek AK, Satija R, Adiconis X, Gertner RS, Gaublomme JT, Raychowdhury R, Schwartz S, Yosef N, Malboeuf C, Lu D, *et al*: Single-cell transcriptomics reveals bimodality in expression and splicing in immune cells. Nature 498: 236-240, 2013.
34. Wills QF, Livak KJ, Tipping AJ, Enver T, Goldson AJ, Sexton DW and Holmes C: Single-cell gene expression analysis reveals genetic associations masked in whole-tissue experiments. Nat Biotechnol 31: 748-752, 2013.
35. Wuhr M, Dumont S, Groen AC, Needleman DJ and Mitchison TJ: How does a millimeter-sized cell find its center? Cell Cycle 8: 1115-1121, 2009.
36. Chew TG, Lorthongpanich C, Ang WX, Knowles BB and Solter D: Symmetric cell division of the mouse zygote requires an actin network. Cytoskeleton (Hoboken) 69: 1040-1046, 2012.
37. Reinsch S and Gonczy P: Mechanisms of nuclear positioning. J Cell Sci 111: 2283-2295, 1998.
38. Gadadhar S, Bodakuntla S, Natarajan K and Janke C: The tubulin code at a glance. J Cell Sci 130: 1347-1353, 2017.
39. Sarkar H, Arya S, Rai U and Majumdar SS: A study of differential expression of testicular genes in various reproductive phases of hemidactylus flaviviridis (Wall Lizard) to derive their association with onset of spermatogenesis and its relevance to mammals. PLoS One 11: e151150, 2016.
40. Thomas DG and Robinson DN: The fifth sense: Mechanosensory regulation of alpha-actinin-4 and its relevance for cancer metastasis. Semin Cell Dev Biol 71: 68-74, 2017.
41. Zhao X, Khurana S, Charkraborty S, Tian Y, Sedor JR, Bruggman LA and Kao HY: α Actinin 4 (ACTN4) regulates glucocorticoid receptor-mediated transactivation and transrepression in podocytes. J Biol Chem 292: 1637-1647, 2017.
42. Hsu KS and Kao HY: Alpha-actinin 4 and tumorigenesis of breast cancer. Vitam Horm 93: 323-351, 2013.
43. Shao H, Wang JH, Pollak MR and Wells A: α-actinin-4 is essential for maintaining the spreading, motility and contractility of fibroblasts. PLoS One 5: e13921, 2010.
44. Hamill KJ, Hopkinson SB, Skalli O and Jones JC: Actinin-4 in keratinocytes regulates motility via an effect on lamellipodia stability and matrix adhesions. FASEB J 27: 546-556, 2013.